

Effect of particle gradation on pullout response of geogrids: A micromechanical perspective

Amrisha Khandelwal^{1,*}, Debayan Bhattacharya¹, J.T. Shahu¹, and Manoj Datta¹

¹Department of Civil Engineering, Indian Institute of Technology Delhi, New Delhi, India

Abstract. Geogrid-soil interface characteristics are essential in designing mechanically stabilised earth walls, reinforced soil slopes, etc. While experimental pullout tests are commonly conducted but it falls short in capturing the micromechanical response. This study employs the 3D Discrete element method (DEM) to simulate the pullout test with biaxial geogrids after validation against the previously reported experimental results. This study primarily focuses on the effect of particle size distribution (PSD), considering both monodisperse and polydisperse systems (well and poorly graded), normal stress, porosity and displacement rates. It was observed that the monodisperse system shows weaker force chains with relatively less particle rotations, resulting in least pullout resistance at macro level when compared against the other two configurations. However, when particle gradations in polydisperse systems are compared, well graded particle assembly shows strong force chain networks than poorly graded which results into maximum pullout resistance at the same pullout displacement. These findings provide valuable micromechanical insights into the underlying role of PSD in optimizing the geogrid-reinforced systems.

1 Introduction

The geogrid-soil interface study is crucial for designing the mechanically stabilized earth (MSE) walls, reinforced soil slopes, pavement applications, etc. This aspect is often investigated through pullout tests, which provide pullout resistance of the geogrid. It is influenced by various soil and geogrid characteristics, however, this study primarily focuses on the effect of PSD, considering both monodisperse and polydisperse systems, normal stress, porosity and displacement rates. Previous studies have demonstrated that particle gradation significantly impacts the mechanical behaviour of geomaterials, including soils and rocks [2]. It also influences packing characteristics, such as porosity and initial conditions, leading to an increased anisotropy within the specimen [2]. Although existing studies primarily examine particle-particle interactions, the effect of gradation on particle-geogrid interaction remains unexplored. This aspect largely remains unexplored and hence calls for a systematic investigation, which has been aimed at in this study.

Unlike traditional experimental pullout tests, this study adopts the numerical framework based on the discrete element method (DEM) to conduct an in-depth analysis of how particle-level kinetics and kinematics affect the overall global (system) response, i.e., the pullout resistance of biaxial geogrid in the granular assembly. The proposed numerical model is first validated against previously reported experimental results. Subsequently, the effects of polydispersity and particle gradation, at three different normal stresses, are explored by considering three distinct PSDs: (i) a monodisperse system with uniform particle size - uniformly graded (UG), (ii) a polydisperse system having poorly graded distribution (PG), and (iii) a polydisperse system having well-graded distribution (WG) with a biaxial geogrid. Furthermore, the influ-

ence of a relatively looser initial packing state, varying normal stress levels, and a range of displacement rates on the pullout response is investigated.

2 Numerical framework for geogrid pullout testing

All numerical simulations in this study have been performed using the open-source Discrete Element Method (DEM) framework, YADE [3]. To validate the DEM model, the experimental results reported by Wang et al. (2016) [1] was selected. The granular assembly was prepared following the PSD reported in [1] (shown in Fig. 1a). The assembly consisted of spherical particles whose particle sizes were upscaled by 2.5 times to enhance the computational efficiency. This scaling approach aligns with previous studies [4]. The uniformity coefficient (C_u) and coefficient of curvature (C_c) for the given distribution are 1.63 and 0.85, respectively, classifying the soil as poorly graded. The input parameters for soil were calibrated using a direct shear test (DST) given in Table 1. The macroscopic internal friction angle obtained from DST was around 41° which closely matches the experimentally reported DST results [1]. The geogrid model used in this study was made of spherocylindrical elements following Anna et al. 2016 [5]. Most of the geogrid pullout DEM studies have adopted the parallel bonded sphere model, however, this approach requires a large number of particles which reduces the computational efficiency and introduces artificial numerical roughness [5]. To maintain consistency with the scaled granular assembly, the rib thickness was also upscaled by a factor of 2.5 [4]. Furthermore, a numerical wide-width tensile test was conducted to calibrate the micromechanical input parameters of geogrid, which are given in Table 1.

The specimen for the pullout test was prepared using multilayer compaction approach, with the geogrid placed at the mid-height of the specimen (i.e., 100 mm). The bulk den-

*e-mail: cez228139@iitd.ac.in

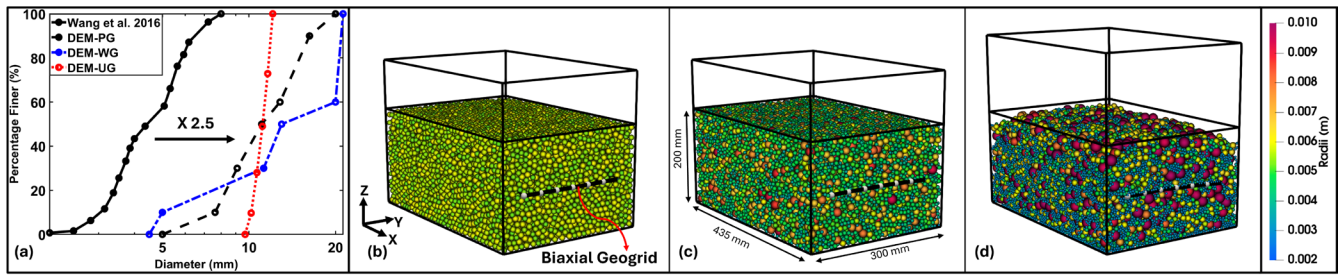


Figure 1. (a) Particle size distribution curves and particle assembly showing (b) Monodisperse-UG specimen, (c) Polydisperse-PG specimen, (d) Polydisperse-WG specimen (For better visibility, refer to online version)

Table 1. Input parameters- calibrated from experimental DST and wide-width tensile test taken from Wang et al. 2016 [1]

Soil	Value
Particle density ρ_s (kg/m ³)	2650
Poisson ratio	1.0
Contact young modulus of the soil E_s (MPa)	100
Contact young modulus of the wall E_w (MPa)	1e6
Particle-particle friction coefficient μ_s	4.0
Particle-wall friction coefficient μ_w	0.8
Damping coefficient	0.3
Geogrid	Value
Particle density ρ_s (kg/m ³)	950
Poisson ratio	1.0
Contact young modulus E_g (MPa)	3000
Normal cohesion (MPa)	400
Shear cohesion (MPa)	300

sity of the assembly was 1.56 g/cm³ with the porosity 41% resulting in approximately 30,400 particles (Fig. 1c). A linear elastic–perfectly plastic contact model was employed for all interactions: particle–particle, geogrid–geogrid, and particle–geogrid [3]. Normal stress was applied at the top boundary by controlling its vertical velocity, and upon reaching the target stress, the geogrid was pulled from the clamped end. The test was terminated when the clamp displacement reached around 20 mm, corresponding to the peak pullout resistance observed in laboratory tests [1]. The influence of displacement rate on the pullout resistance was studied. Numerical simulations were conducted on four different displacement rates - 0.001 m/s, 0.01 m/s, 0.05 m/s and 0.1 m/s (Fig. 2). This investigation reveals that the peak pullout resistance remains relatively unchanged for displacement below 5 mm. However,

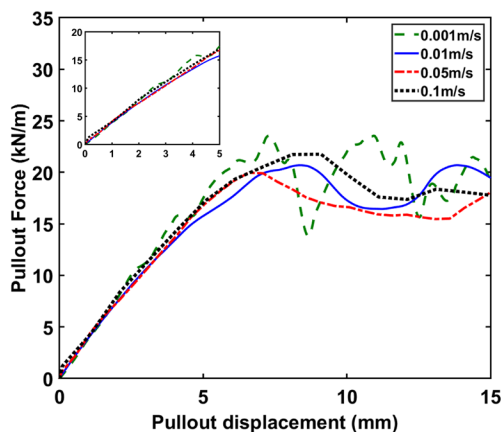


Figure 2. Influence of displacement rate on pullout resistance of PG assembly at 20 kPa

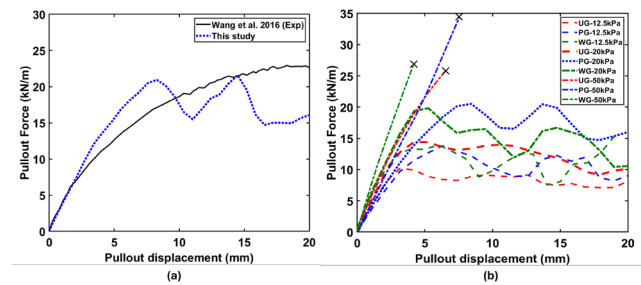


Figure 3. (a) Validation of pullout test (after [1]) at 20 kPa normal stress (b) Effect of normal stress on pullout resistance for different particle gradation assemblies

beyond this threshold value, the variations in pullout resistance are observed due to the stick-slip phenomenon [6]. Notably, increasing the displacement rate beyond 0.01 m/s results in significantly higher computational time without any significant noticeable change hence, it offers an optimal choice of balancing the computational efficiency without affecting the numerical accuracy of the results in the present analysis.

The validation of the pullout test after [1] is shown in Fig. 3a. The numerical results reveal a peak pullout resistance that shows a similar trend to that obtained experimentally. The fluctuations depicted in Fig 3a. represent the characteristic stick-slip behavior, which has been documented in previous studies as well [6]. These fluctuations are often amplified in numerical simulations due to the discrete nature of the modeling approach and are not merely numerical artefacts. However, the peak occurs earlier in the numerical simulations as compared to the experimental results. This observed behaviour is primarily due to the use of relatively rigid, spherical particles and the chosen contact model (linearly elastic perfectly plastic). Despite this assumption, a closer investigation of the micromechanical responses at a displacement of 5 mm provides valuable insights on the kinetics and kinematics at the geogrid-soil interface, thereby supporting the validity of the selected micromechanical parameters and reinforcing the overall reliability of this study. Further, the numerical study is being carried out within the realms of the discrete granular setting, which tries to mimic the experimental conditions that represents a continuum perspective in reality.

3 Influence of particle gradation on macroscopic response

Fig. 1a shows the PSD of the gradations considered in this study. C_u and C_c values of UG and WG are 1 & 1 and 4 &

1.27 respectively. WG assembly (Fig. 1d) consists of 48,000 particles while 21,600 particles are there in the UG specimen (Fig. 1b), with an initial porosity of 41% in both cases. Fig. 3b presents pullout test results for all gradations (UG, PG, WG) at three normal stresses- 12.5 kPa, 20 kPa and 50kPa. It is observed that UG exhibits lowest peak pullout resistance than both polydisperse systems across all normal stresses. At high normal stresses, the peak pullout resistance is not achieved due to rupture of the geogrid; the ‘x’ indicates the breakage point of the geogrid. The variation observed across all gradations remains similar at different normal stresses i.e., WG reaches its peak pullout resistance earlier than PG followed by UG. Pullout resistance increases with normal stress. At low normal stresses, particles can move and readjust amongst themselves more easily, resulting in a reduced pullout resistance, while the particle movement gets relatively restrained at higher normal stresses resulting in a higher pullout resistance of the geogrid.

4 Microscopic responses

This section attempts to bridge the gap between macroscopic and microscopic responses through observed kinetics and kinematics of the geogrid-pullout test in various PSD configurations. The micro responses are plotted at 0 mm and 5 mm pullout displacements for all gradations (UG, PG, WG) at 20 kPa.

4.1 Kinematics at interface

This section reveals the kinematic behavior at the soil-geogrid interface using polar histograms (Fig. 4). To quantify the directionality of particles, a second-order Fourier analysis was employed [7], characterised by two parameters- the degree of anisotropy (a) and the principal orientation (θ). Due to the symmetry observed in the contact normal orientations both above and below the geogrid, the present analysis focuses solely on the lower portion of the assembly for brevity of the article. The Fourier series expansion of the probability density function is expressed as:

$$E(\theta) = \frac{1}{2\pi} [1 + a \cos 2(\theta - \theta_n)] \quad (1)$$

where $E(\theta)$ represents the contact normal distribution function, (θ) is the inclination of contact normal from the reference axis, (a) is the second-order coefficient indicating degree of contact normal anisotropy, and (θ_n) is the principal orientation of fabric anisotropy [7]. Fig. 4a, 4c, and 4e illustrate the contact normal orientations for UG, PG, and WG at the initial state ($u = 0$ mm). At this stage, the granular assembly exhibits inherent anisotropy as evidenced by high a value (Table 2), and the characteristic peanut-shaped distribution since the particles are aligned along the vertical (Z) axis, $\theta \approx 90^\circ$. This is because the specimen was prepared using the gravity deposition method. During the pullout process, at $u = 5$ mm, a decreases in all gradations, and the particles tend to align in their preferred direction of the pullout, as depicted by an increase in θ as shown in Fig. 4b, 4d and 4f for UG, PG and WG respectively. Notably, the particles exhibit rotations of approximately 17° , 37° and 35° for UG, PG, and WG, respectively. Large-sized particles (UG) exhibit least rotation compared to the other two cases (WG and PG), which contain a mix of relatively large and smaller particles. This suggests that smaller particles predominantly undergo rotation, while

larger particles primarily translation. Furthermore, although WG and PG show similar trends of rotation, the number of particles experiencing strong contact forces is higher in WG than in the PG assembly, which correlates with the observed increase in global pullout resistance (see Fig. 3b).

Furthermore, to gain deeper insight into the fabric anisotropy, principal fabric estimates (ϕ_1, ϕ_2) are calculated using the second-order fabric tensor, defined by:

$$\begin{pmatrix} \Phi_{xx} & \Phi_{xy} \\ \Phi_{yx} & \Phi_{yy} \end{pmatrix} = \frac{1}{N_c} \begin{pmatrix} \sum_{j=1}^{N_c} n_x^p n_x^p & \sum_{j=1}^{N_c} n_x^p n_y^p \\ \sum_{j=1}^{N_c} n_y^p n_x^p & \sum_{j=1}^{N_c} n_y^p n_y^p \end{pmatrix} \quad (2)$$

where N_c is the total number of contacts, and $\mathbf{n}^p = (n_x^p, n_y^p)$ represents the unit normal vector at the p^{th} contact. Table 2 revealed that a derived from Fourier analysis is closely aligned with $2(\phi_1 - \phi_2)$ computed from second-order fabric tensor [7]. This correlation validates the consistency of the two methods in characterizing the directional fabric of the granular assembly, employing their effectiveness in quantifying the fabric anisotropy.

Table 2. Degree of Anisotropy and principal fabric orientation using second-order Fourier fit and second-order fabric tensor at pullout displacement of 0 mm and 5 mm

Gradation	Uniformly graded		Poorly graded		Well graded	
	0mm	5mm	0mm	5mm	0mm	5mm
Parameters						
Degree of anisotropy (a)	1.36	0.37	0.95	0.50	0.53	0.39
Principal Orientation (θ)	88°	105°	89°	126°	88°	124°
Major principal fabric (ϕ_1)	0.74	0.42	0.58	0.46	0.47	0.43
Minor principal fabric (ϕ_2)	0.14	0.29	0.21	0.26	0.26	0.28
$2(\phi_1 - \phi_2)$	1.2	0.3	0.7	0.4	0.4	0.3

4.2 Kinetics at interface

The interparticle forces within the assembly has been represented by the network of contact force chains, shown in Fig. 4a-4f for each gradation at a pullout displacement of 0 mm and 5 mm. The force chains are depicted in the XZ plane (sectional elevation) and the contact normal forces below 2% of the maximum value are omitted to enhance visibility. The line thickness corresponds to the magnitude of the contact normal forces. These force chains reorient towards the pullout direction (along X-direction), forming V-shaped patterns around the geogrid. At $u = 5$ mm, Figs. 4b, 4d, and 4f clearly show that WG develops the strongest force chain network, followed by PG and UG, consistent with the higher pullout resistance. The delayed peak of the UG is attributed to its weak force chain network accumulated more near front wall, hence, less effective stress redistribution within the granular ensemble.

The tensile forces along the geogrid length for all gradations (UG, PG, WG) at $u = 5$ mm is shown in Fig. 4h, 4i, 4j. The force distribution clearly exhibits a nonlinear behavior. It is evident that for the same pullout displacement, the force distribution along the geogrid varies significantly depending on the particle size distribution. The tensile force exhibits highest value in case of WG, followed by PG and UG, which follows the pattern of the global response because of greater interlocking provided by the particulate assembly. This is further cor-

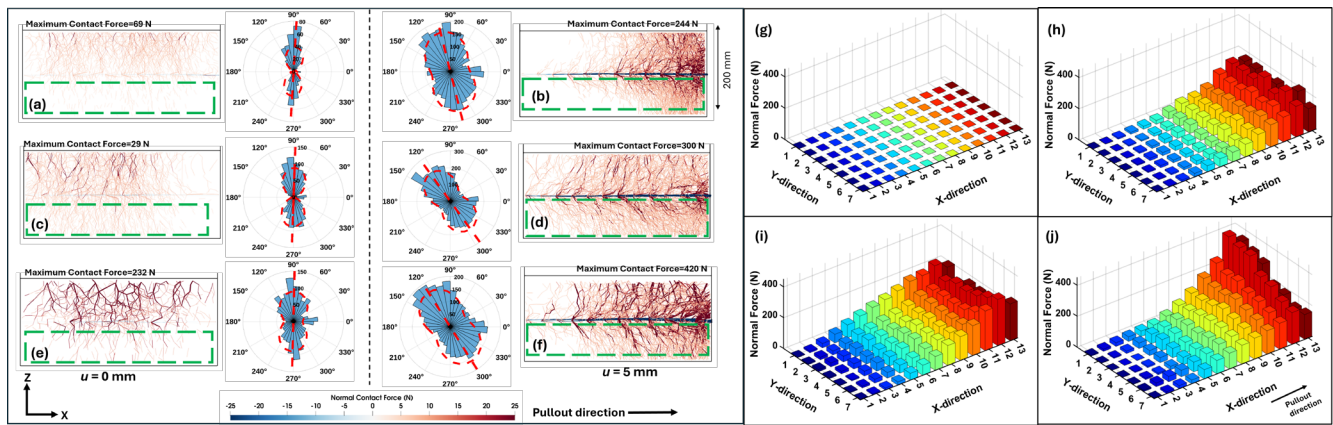


Figure 4. Force chains (FC), contact normal orientations (CN) in assembly and tensile forces (TF) along geogrid (a) FC and CN of UG at $u=0$ mm and (b) at $u=4$ mm (c) FC and CN of PG at $u=0$ mm and (d) at $u=4$ mm (e) FC and CN of WG at $u=0$ mm and (f) at $u=4$ mm (g) TF at $u=0$ mm for all assemblies (h) TF for UG at $u=5$ mm (i) TF for PG at $u=5$ mm (j) TF for WG at $u=5$ mm (For better visibility refer to online version)

robored by the observed force chain patterns in Fig. 4b, 4d and 4f.

5 Effect of soil porosity

Porosity (η) is varied from 41% to 46%, representing a relatively looser material state as shown in fig. 5. The relatively looser state of granular ensemble results in reduced pullout resistance as compared to a denser state (Fig. 5) this observed material response may be attributed to the particulate kinematics. The loosely packed granular media ($\eta = 46\%$) can undergo translation more easily in the direction of pullout, leading to a decreased resistance as compared to the relatively denser ensemble ($\eta = 41\%$).

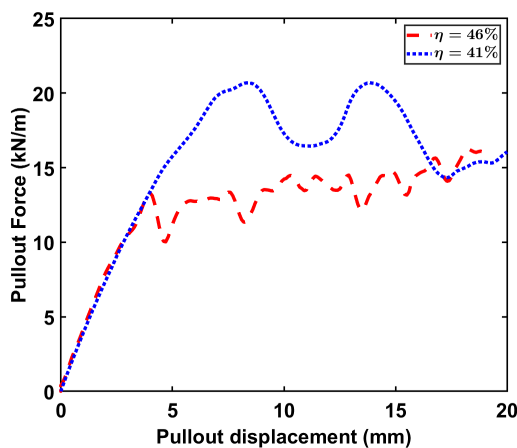


Figure 5. Influence of displacement rate on pullout resistance of PG assembly at 20 kPa

6 Conclusion

This study investigates the micromechanical behaviour of soil-geogrid interface with the aid of an open-source 3D Discrete Element Method (DEM) framework, YADE, to perform pullout tests under different particle gradations with biaxial geogrid at three normal stresses. Furthermore, effect of relatively looser material state in poorly graded at 20 kPa was also investigated. The following conclusions are drawn from this study:

- At a particular pullout displacement, monodisperse system, compared to polydisperse granular ensemble exhibits relatively less particle rotation while particle translations significantly higher at the microscale level. This weakens the force chain networks within the granular assembly, thus resulting in the lowest pullout resistance at macroscale.
- Among polydisperse systems, when comparing different particle gradations at a particular pullout displacement, well graded and poorly graded specimens exhibit almost similar particle rotations but the force chain networks in well graded are stronger, leading to a higher pullout resistance at global level.
- Relatively looser material state undergoes translation easily hence, offers less pullout resistance as compared to denser material state

References

- [1] Z. Wang, F. Jacobs, & M. Ziegler, *Geotextiles and Geomembranes*, 44(3), 230-246 (2016). <https://doi.org/10.1016/j.geotextmem.2015.11.001>
- [2] M. S. Basson, A. Martinez, & J. T. DeJong, *Jour. of Geotech. and Geoenviron. Eng.*, 150(8), 04024060 (2024). <https://doi.org/10.1061/JGGEFK.GTENG-12310>
- [3] V. Šmilauer et al. (2021) *Yade Documentation 3rd ed. The Yade Project*. 10.5281/zenodo.5705394. <http://yade-dem.org>
- [4] Z. Wang, Q. Xia, G. Yang, W. Zhang, & G. Zhang, *Geotextiles and Geomembranes*, 51(4), 72-84 (2023). <https://doi.org/10.1016/j.geotextmem.2023.03.005>
- [5] A. Effeindzourou, B. Chareyre, K. Thoeni, A. Giacomini, & F. Kneib, *Geotextiles and Geomembranes*, 44(2), 143-156 (2016). <https://doi.org/10.1016/j.geotextmem.2015.07.015>
- [6] A. Pant, M. Datta, G. V. Ramana, & D. Bansal, *Measurement*, 148, 106944 (2019). <https://doi.org/10.1016/j.measurement.2019.106944>
- [7] D. Bhattacharya, R. Kawamoto, K. Karapiperis, J. E. Andrade, & A. Prashant, *Acta Geotechnica*, 16, 113-132 (2021). <https://doi.org/10.1007/s11440-020-00996-8>